Chapter 8
A Basic Overview of Fuel Cells: Thermodynamics and Cell Efficiency

Narcis Duteanu, Adriana Balasoiu, Pritha Chatterjee and Makarand M. Ghangrekar

Abstract In the last century, there has been rapid urbanization leading to increased energy demand with an ever increasing load on nonrenewable resources and subsequent escalation of pollution. A viable solution to these two problems can be a power supply technology that is able to produce energy with minimum or zero pollutant emission into the environment. Fuel cells appear to be an eco-friendly power supply technology. Main advantage of fuel cell technology is represented by direct conversion of fuels into electrical energy, with zero emissions, when hydrogen is used as fuel. This article describes the basic overview of fuel cell technology in order to better understand the construction and also the working principle of this eco-friendly technology.

1 What Is a Fuel Cell?

Fuel cells (FC) appear as a *sci fi* system and represent a device able to convert the chemical energy of a fuel directly into electrical energy [1–3], and it is characterized by the continuous feed with active chemical species to undergo redox reactions [4]. In classical energy production technologies, fuel is burned to generate heat, which is further converted to steam in a steam engine. Produced steam is used to drive a

N. Duteanu (✉) · A. Balasoiu
CAICAM, Faculty of Industrial Chemistry and Environmental Engineering, Politehnica University of Timisoara, 6, Pirvan Street, 300223 Timisoara, Romania
e-mail: narcis.duteanu@upt.ro

A. Balasoiu
e-mail: adriana.balasoiu@ymail.com

P. Chatterjee · M.M. Ghangrekar
Department of Civil Engineering, Indian Institute of Technology Kharagpur, Kharagpur 721302, India
e-mail: pritha.besu@gmail.com

M.M. Ghangrekar
e-mail: ghangrekar@civil.iitkgp.ernet.in

© Springer International Publishing AG 2017

Inamuddin et al. (eds.), *Organic–Inorganic Composite Polymer Electrolyte Membranes*, DOI 10.1007/978-3-319-52739-0_8

turbine which converts the thermal energy present in steam to mechanical energy. Finally, the mechanical energy is converted to electrical energy using a generator [1].

In a fuel cell, electricity is produced directly by burning of fuel, hence the intermediate steps of production of heat and mechanical energy can be avoided. This helps to evade the thermodynamic limitation of any engine. This thermodynamic limitation is known as Carnot efficiency which is defined as the upper limit on the efficiency that any classical thermodynamic engine can achieve during the conversion of heat into work [5]. Since the fuel cell system does not have to go through the Carnot cycle, hence its efficiency is expected to be higher than classical heat engines.

Combustion of fuels in conventional energy producing technologies has a huge environmental impact. However in a fuel cell, electrochemical conversion of the chemical energy, in presence of catalyst, present in the bonds of the fuel into electrical energy, produces power with minimal or zero pollution. In comparison with batteries, fuel cells are able to produce electricity as long as the fuel and also the oxidant are continuously replenished at anode and cathode, respectively [5, 6].

2 Fuel Cell Structure and Classification

A single unit cell represents core of FC which consists of two electrodes and one electrolyte layer. Anode (negative electrode) is placed in contact with electrolyte layer on one side and the cathode (positive electrode) is placed in contact on the other side of the electrolyte [5, 6]. A schematic representation of a classical H_2/O_2 fuel cell is presented in Fig. 1. Starting from a fuel cell basic unit, stacks are developed where individual core units are modularly combined in order to deliver the desired output current and voltage [6].

Fuel cells are able to process a wide variety of fuels, such as hydrogen, hydrocarbons, alcohols, natural gas, and derivatives. Burning of fossil fuels in conventional energy producing technologies has a high global warming potential due to emission of greenhouse gases and a high environmental impact due to use of nonrenewable fuels. Taking into account, the lower global warming potential by reducing greenhouse gases emissions, FC using hydrogen, are becoming more and more attractive. In all classical FC, during electricity production, anode must be fed continuously with the fuel, and simultaneously the cathode must be furnished continuously with an oxidant, preferably oxygen from air. Electricity generation from the FC is due to the spontaneous anodic and cathodic half-cell reactions [1, 4, 6, 7]. In a hydrogen fuel cell, at the anode catalyst layer, hydrogen undergoes an oxidation reaction producing protons and electrons. The generated protons are then conducted by the electrolyte membrane and delivered at the cathode, where they participate in reduction reaction along with oxygen and electrons, which traverse through the external electrical circuit producing water (Fig. 1).

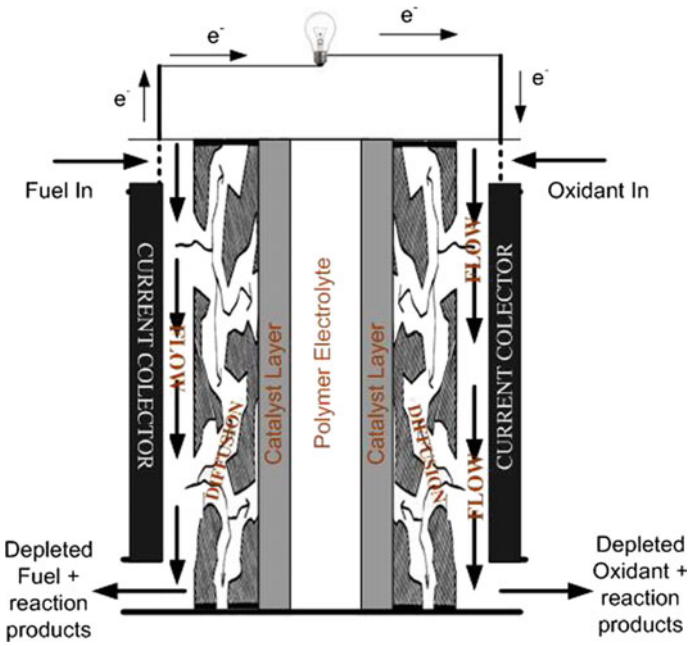

Fig. 1 Working principle of PEMFC

Fuel cells can be classified either based on operating temperature [4] or more commonly by the electrolyte used [1, 4, 6, 8]. Based on electrolyte used fuels cells are classified as follows [1, 4, 6, 8–12]:

- Proton Exchange Membrane Fuel Cells (PEMFC) or polymer electrolyte fuel cell:
  - H_2/O_2 PEMFC;
  - **D**irect **M**ethanol **F**uel **C**ells (**DMFC**);
  - **D**irect **E**thanol **F**uel **C**ells (**DEFC**);
  - **D**irect **F**ormic **A**cid **F**uel **C**ells (**DFAFC**);
  - **D**irect **B**orohydride **F**uel **C**ells (**DBFC**).
- **A**lkaline **F**uel **C**ells (**AFC**):
  - **P**roton **C**eramic **F**uel **C**ell (**PCFC**);
  - **D**irect **B**orohydride **F**uel **C**ell (**DBFC**);
  - **D**irect **A**lcohol **F**uel **C**ell (**DAFC**).
- **P**hosphoric **A**cid **F**uel **C**ell (**PAFC**);
- **M**olten **C**arbonate **F**uel **C**ells (**MCFC**);
- **S**olid **O**xide **F**uel **C**ells (**SOFC**);
- **D**irect **C**arbon **F**uel **C**ells (**DCFC**).

Based on operating temperature, fuel cells can be classified as:

- Low-operating temperature fuel cell (50–250 °C): PEMFC, AFC, PAFC;
- High-operating temperature fuel cell (650–1000 °C): MCFC, SOFC, DCFC.

3 Fuel Cell Construction

Polymer electrolyte fuel cells are constructed by using a Membrane Electrode Assembly (MEA). In all cases, MEA is formed from a central polymer electrolyte (membrane) and two electrodes on either side of the membrane [13–18]. By placing the two electrodes very close, it is expected to improve the cell performance by reducing the internal resistance of electrolyte. Schematically the core of any PEMFC can be represented as in Fig. 2.

To obtain a higher efficiency, it is necessary to have a strong contact between the catalyst layer and the polymer electrolyte membrane. This represents the most critical and important portion of a FC and is called the three phase interface, where the electrocatalytic reactions take place [4, 6, 16, 17, 19]. A catalyst particle can be active for the electrochemical reactions only if it is in contact with the reactants, electrolyte and also with the electrode [4, 20–23]. Contact of catalyst layer with electrolyte is necessary in order to be able to get the ionic reaction product from

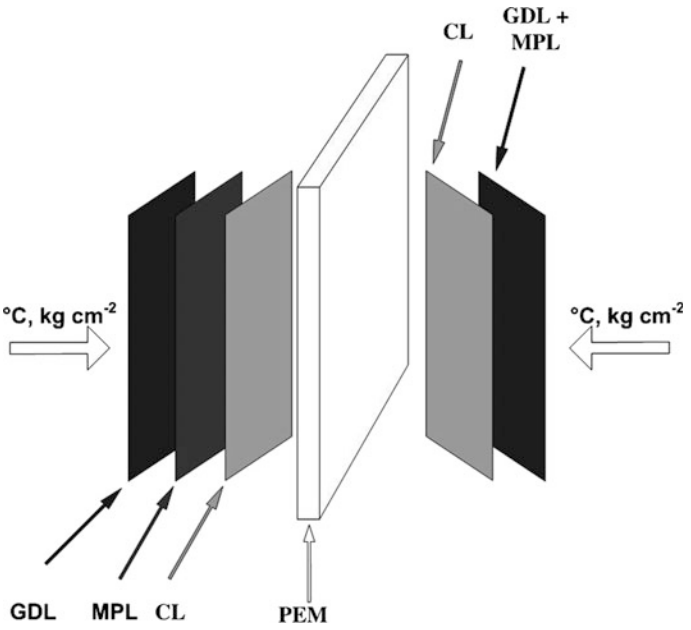

Fig. 2 Schematic representation of MEA production

production site and conduct them into the consumption place, and at the same time electrical contact with solid electrode is needed in order to retrieve electrons [24, 25]. Also to enhance reaction rate, sufficient catalyst should be present on the electrodes [4, 6]. This can be achieved either by applying a high catalyst loading rate or using a small quantity of electrolyte per cell [14, 26].

A practical method used to increase the electrocatalytic surface area of the electrode, along with reduction of catalyst loading, is by usage of 3D structured catalyst layers. Such 3D structures can be produced by using catalyst nanoparticles supported on the surface of some larger support particles. In actual stage of development carbon particles with sizes of around 10 nm, [13, 16, 27–31], carbon nanofibers [28, 29, 32–36] and graphene [37] are used as support particles.

Platinum is the most commonly used catalyst for hydrogen oxidation and oxygen reduction reactions (ORR) [13, 14, 20, 29–31, 36, 38–43]. However, platinum is expensive, and hence to reduce the cost of fuel cell without compromising with the performance, it is necessary to use nanoparticles of catalyst on support particles [1, 6, 22, 29, 33, 44–51], which increases the active surface area available for reactions. Increased surface area helps in improved reactant and products transport to and from bulk to the three phase interface [18, 25, 52, 53].

As can be seen from Fig. 2, electrode used in a fuel cell construction is a complex structure consisting of a gas diffusion layer, a microporous layer, and a catalyst layer [52]. One of the most important part of MEA is represented by the gas diffusion layer (GDL), which provides durability to the entire assembly and at the same time should ensure proper electrical contact between catalyst layer and the current collectors [52–55]. Presence of GDL increases contact resistance at the interface between the GDL and current collectors, which reduces energy conversion efficiency. At the same time, it is important to obtain a porous structure of GDL in order to be able to have continuous reactant and product flow to and from the catalyst layer to the bulk liquid [25, 53, 56]. Maximum power can be achieved only if the GDL present optimum hydrophobicity in order to remove produced water from the catalyst layer. Water retention is equivalent to blockage of internal channels, leading to a limitation of the supply of reactant and inefficient transport of reaction products, thus reducing the fuel cell efficiency [52–60]. Graphite paper consisting of woven carbon fibers is the most commonly used GDL (Fig. 3). This mesh of carbon fibers forms a series of interconnected channel like structure, which allows efficient transport of reactants and products. Hydrophobic layer on the graphite paper links the individual carbon fibers together.

The microporous layer (MPL), located between GDL and catalyst layer have the following features [61]:

- assures a physical microporous base for catalyst layer, which helps in transportation of products and reactants to and from the catalyst layer;
- prevents penetration of catalyst particles inside the GDL;
- plays an important role in electrode water management;
- reduces the contact resistance between catalyst layer and the GDL.

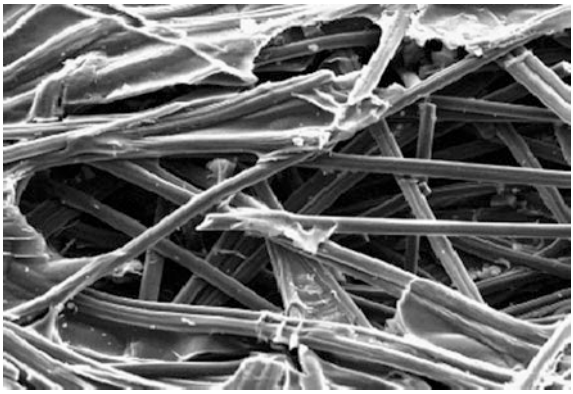

Fig. 3 SEM obtained for commercial carbon paper with 20% wet-proof at 500 X magnification

In short, MPL is responsible for rapid removal of reaction products, and reduction of water accumulation inside the electrode. In this way, it avoids blockage of catalyst layer with water molecule and reaction products.

Water management inside electrodes can be done by using hydrophobic/hydrophilic organic compounds (such as PTFE or Nafion 117) [20, 50, 52, 54, 55, 58, 62]. PTFE or Nafion should be used in an optimum loading because higher loading increases the internal resistance of the MPL and limits porosity (number and diameter) thus causing mass transfer limitations inside the electrode [20, 58, 63, 64]. All these secondary effects in turn reduces the efficiency of fuel cells [20, 55, 58–60, 62].

To improve fuel cell efficiency, internal resistance of the cell should be reduced. Internal resistance of MPL is dependent on the MPL thickness and the internal resistance of a gas diffusion electrode decreases when the MPL thickness is reduced [20, 54, 55, 59, 60]. However, excessive reduction of MPL or GDL thickness will cause faulty water management and corrosion of catalyst layer [18, 25, 53, 65, 66]. Hence, an optimum thickness of the MPL or GDL should be used.

The catalyst layer forms the most active part of a fuel cell. It should have maximum active surface area with minimum catalyst loading. Platinum is the most commonly and efficiently used catalyst material in a fuel cell; however, its high cost and instability at alkaline pH limits its extensive use. Other than high reactive surface area, catalyst layer should have proper water management to prevent blockage or dryness of the membrane.

Hydrophobic polytetrafluoroethylene (PTFE) was first developed by Union Carbide in the year 1960, which was used as binder and GDL in membrane electrode assembly of a fuel cell [26, 61, 67, 68]. Later on, PTFE was substituted by hydrophilic perfluorosulphonic acid. PTFE or perfluorosulphonic acid is used to enhance contact between electrolyte and catalyst layer and optimize water retention inside the MEA. A membrane electrode assembly should have efficient proton transfer ability, transporting protons from anode through the membrane to the cathode for oxygen reduction. This property can be achieved by using Nafion ionomer or other proton exchanging compounds in the catalyst layers.

Use of proton conducting compounds improves charge transfer efficiency thereby reducing the need of higher catalyst loading; hence, reducing cost of fuel cells [13, 20, 26, 61, 69–72].

Recent research has mainly focused on developing cheaper and effective catalysts. Binary or tertiary alloys or metal oxides are majorly used recently as a substitute for platinum [26, 62, 64, 70, 73–83]. Oxygen reduction reaction can be conducted via two different pathways (a) two electron pathway forming water, (b) four electron pathway producing hydrogen peroxide. The two electron pathway is more desirable because prolonged exposure to hydrogen peroxide reduces durability and structural integrity of the membrane [83, 84]. Hence, while choosing a catalyst, it is important to know the mechanism of the reaction it supports.

Solid polymer electrolyte or proton exchange membrane (PEM) is important in fuel cell as it allows only the proton to be transported through it and not the electrons [15, 38, 85–89]. Nafion 117 is the most commonly used proton exchange membrane, which is a polyfluorinated polymer with sulfonic groups as proton donors/acceptors. High chemical and thermal stability (can be used for short time at 140 °C), along with good ionic conductivity makes Nafion such a popular choice for PEM. Presence of sulfonic group that has an ionic bond between oxygen and proton in the Nafion is responsible for its ionic conductivity. Water can penetrate into the space between the polymeric chains thus giving the protons a high mobility. N117 membrane is also able to conduct ions in alkaline media by exchanging the protons present in the sulfonic group with sodium ions which are mobile in the alkaline fuel cells. Main characteristics of N117 membrane are presented in Table 1 [90].

DuPont is the major producer of these Nafion membranes, which should be given a pretreatment as mentioned below before use in a PEMFC:

1. treatment with 3% H_2O_2 for at least 30 min in order to eliminate all possible organic residues from inside of the membrane;
2. cleaning of the treated membrane with distilled water;
3. treatment with 1 M H_2SO_4 solution for at least 1 h, in order to obtain the membrane in "H" form, when protons are linked onto the SO_3^- groups;
4. cleaning with distilled water.

To use the membrane in alkaline media, the protons in the sulphonic group in the membrane should be replaced by sodium ions prior to use by boiling the N117 membrane for at least 1 h in 0.5 M NaOH solution [91, 92]. While using in a fuel

Table 1 Characteristics of Nafion 117

Main polymeric chain	Perfluorosulfonic polymer (PFSA polymer acid)
Active group	H^+
Thickness (μm)	183
Conductivity (S cm^{-2})	0–10
Acidity (meq g^{-1})	>90
Maximum working temperature (°C)	140
Working pH	2–11

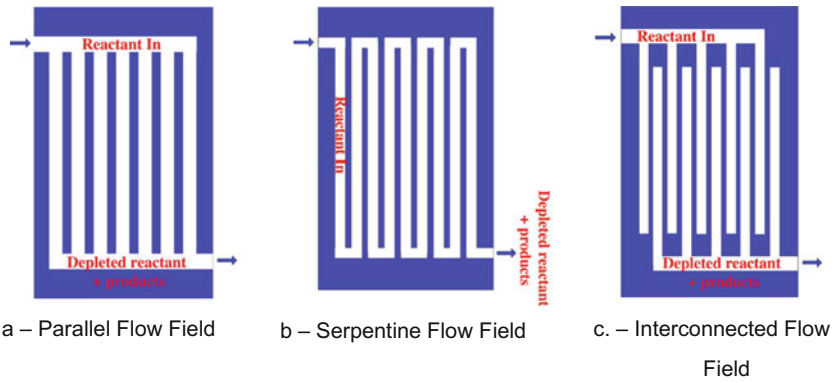

Fig. 4 Usual flow-fields used in PEMFC construction

cell, it is also possible to replace the protons with Na by recirculation of alkaline solution in the fuel cell for some time.

To achieve interconnected or stacked fuel cell, proper design and development of gas diffusion electrode is necessary. Reactants are supplied at the GDL from which it reaches the active catalyst sites by diffusion through GDL and MPL. Reactants can be supplied by using flow-fields technique, which also removes reaction products and ensures electrical contact, in order to collect and transport electrons into the external circuit [93, 94]. Design and construction of flow-fields have been modified from the day of inception when simple parallel channels drilled into graphite plates were used [64, 88, 94]. Later on the simple parallel channels were modified into serpentine and interconnected structures. Figure 4 shows a schematic representation of the different types of flow-fields.

When the reactants are transported from the inlet to the outlet of the flow-fields, there is a considerable pressure drop, hence the catalyst layer near the outlet is not optimally utilized, thus necessitating improved and modified design of flow-fields to reduce pressure drop. Rostami et al. [95] demonstrated that pressure drop observed along the flow-field channel is accompanied by the appearance of a reverse pressure drop responsible for more losses inside the channels [96–98]. Friction between reactant molecules and the walls of the flow-field, or with the internal channel of gas diffusive electrodes cause pressure drop [1, 4, 88, 99]. Inefficient transfer of water produced in the active catalyst sites causes blockage of channels, reactants are diverted to the neighboring channels, which also contribute to internal pressure loss.

When the cell is flooded, water blocks the passage of gases through the flow channels; thus causing mass transport limitation which in turn reduces fuel cell efficiency [1, 4, 100, 101]. Barbir et al. used pressure drop as a diagnostic tool for fuel cell flooding, co-relating it with presence of liquid water inside the cathode channels [99, 102]. With time, design of flow-fields are being further modified to more complex structures, reducing pressure drops to improve performance of fuel cells [88, 99, 103–105].

4 PEMFC Types, Electrode Reactions, and Cell Potential

4.1 H_2/O_2 PEMFC

This particular type of fuel cell was developed in 1963 by General Electric for the space mission Gemini. This cell was fueled with pure hydrogen and pure oxygen, and delivered a maximum power of 1 kW [34]. The following reactions take place at the electrodes:

Anode (−)	$H_2 \rightarrow 2\,H^+ + 2e^-$	$E_a^0 = 0.\,V$
Cathode (+)	$1/2\,O_2 + 2H^+ + 2e^- \rightarrow H_2O$	$E_c^0 = 1.229\,V$
Overall reaction:	$H_2 + 1/2\,O_2 \rightarrow H_2O$	$U^0 = 1.22\,V$

4.2 Direct Methanol Fuel Cells (DMFC)

Direct methanol fuel cells are a subset of polymer electrolyte fuel cells which are able to directly convert the chemical energy stored in methanol to electrical energy. Methanol can be easily transported using similar network like gasoline transport, thus making DMFC advantageous. As compared to PEMFC fueled with hydrogen, DMFC gives a lower power output and lower efficiency due to slow reaction kinetics of methanol oxidation and methanol crossover from the anodic chamber to cathode [106, 107]. Crossover of methanol from anode to cathode becomes the limiting factor when methanol concentration is above 2 M, and it is oxidized at the cathode leading to decreased performance of the cell [108]. Proper care should be taken while handling DMFC as methanol vapors are toxic [108, 109]. The following reactions take place at the anode and cathode of a DMFC:

Anode (−)	$CH_3OH + H_2O \rightarrow CO_2 + 6H^+ + 6e^-$	$E_a^0 = 0.02\,V$
Cathode (+)	$3/2\,O_2 + 6H^+ + 6e^- \rightarrow 3H_2O$	$E_c^0 = 1.23\,V$
Overall reaction:	$CH_3OH + 3/2O_2 \rightarrow CO_2 + 2H_2O$	$E_{cell} = 1.21\,V$

4.3 Direct Ethanol Fuel Cells (DEFC)

As DMFC, the direct ethanol fuel cells are also a subset of PEMFC which are able to directly convert ethanol into energy. Usage of ethanol as fuel is attractive because it is a nontoxic compound, which can be supplied by using the infrastructure used for petrol products distribution and can also be produced from food and nonedible crop residues in an environment friendly way [40, 71, 110, 111]. Low crossover of ethanol as compared to methanol, because of bigger molecule size (smaller permeability) is another advantage of DEFC [26, 110, 111]. Though ethanol oxidation

is slow reaction, but reaction kinetics of both ethanol oxidation at anode and oxygen reduction at cathode can be improved by replacing acidic anodic media with an alkaline one [110]. This improved kinetics of oxygen reduction into the alkaline media was experimentally demonstrated by An et al. [112], Modestov et al. [113, 114], and An et al. [115] by comparative tests using classical acidic fuel cells and also alkaline one. An et al. [39, 116] suggested a direct ethanol fuel cell combining acidic and alkaline fuel cells, with alkaline anodic media and an acidic cathodic media.

In classical system, the following reactions take place in acidic media at the electrode in a DEFC:

Anode (−)	$CH_3CH_2OH + 3H_2O \rightarrow 2CO_2 + 12H^+ + 12e$	$E_a^0 = 0.085\,V$
Cathode (+)	$3O_2 + 12H^+ + 12e^- \rightarrow 6H_2O$	$E_c^0 = 1.229\,V$
Overall reaction:	$CH_3CH_2OH + 3O_2 \rightarrow 2CO_2 + 3H_2O$	$E_{cell} = 1.144\,V$

4.4 Direct Formic Acid Fuel Cells (DFAFC)

Direct formic acid fuel cells are becoming more and more attractive because of their high power output, which is a result of higher open circuit potential, correlated with faster kinetics of formic acid oxidation [117–119] and also with low crossover rate of formic acid [118, 120] than direct methanol fuel cells. Due to smaller number of electrons exchanged during formic acid oxidation, crossover of formic acid is only 50% as compared to methanol [108]. In case of usage of formic acid as fuel into a classical PEMFC, the semi-reactions are as follows [108]:

Anode (−)	$CHOOH \rightarrow CO_2 + 2H^+ + 2e^-$	$E_a^0 = 0.25\,V$
Cathode (+)	$1/2\,O_2 + 2\,H^+ + 2e^- \rightarrow H_2O$	$E_c^0 = 1.229\,V$
Overall reaction:	$CHOOH + 1/2O_2 \rightarrow CO_2 + H_2O$	$E_{cell} = 1.479\,V$

4.5 Direct Borohydride Fuel Cells (DBFCs)

DBFCs were developed in 1960 by Snyder and Irving [48]. Due to high energy density, sodium borohydride represents a potential fuel for direct electro-oxidation in DBFC [121]. Nontoxic by-products obtained from anodic oxidation of BH_4^- are major advantage of DBFC [45, 48]. Borohydride being a stable solid compound, it is easy to store and transport [79]. In addition, during electrochemical oxidation of borohydride CO_2 is not produced and also the catalytic activity is not affected because no CO intermediates are produced during the oxidation process [45, 79]. Borohydride, however, is not stable in acidic media and hence during operation of DBFC, a strong alkaline media is required to be used [45, 79, 121]. Among the

different types of PEMFC, direct borohydride fuel cell generates maximum potential. When oxygen is used as oxidant, the half-cell reactions in a DBFC are as follows [121]:

Anode (−)	$BH_4^- + 8HO^- \rightarrow BO_2^- + 6H_2O + 8e^-$	$E_a^0 = -1.24\,V$
Cathode (+)	$2O_2 + 4H_2O + 8e^- \rightarrow H_2O$	$E_c^0 = 0.40\,V$
Overall reaction:	$BH_4^- + 2O_2 \rightarrow BO_2^- + H_2O$	$E_{cell} = 1.64\,V$

5 Fuel Cell Thermodynamics

Like any other energy converting device, fuel cell follows the second law of thermodynamics [1, 4, 6]. The electrode reactions are taking place at interface of the electrode–electrolyte, where three different phases are in contact: electrolyte, electrode (catalyst layer), and reactant (fuel or oxidant). The cathodic and anodic reactions take place simultaneously during power production [1, 2, 4–6, 9, 11, 38, 87]. To have a better understanding of fuel cell functioning, it is important to consider both thermodynamic and kinetic aspects [1, 4, 6, 12].

Let us consider that the fuel cell overall reaction is:

$$aA + bB \rightarrow cC + dD$$

For the above reaction, Gibbs free energy is calculated by using following Eq. 1.

$$\Delta G = c\mu_c + d\mu_d - a\mu_a - b\mu_b \tag{1}$$

where μ_c, μ_d, chemical potentials of reaction products, and μ_a, μ_b, chemical potentials of reactants. Chemical potential can be calculated as (Eq. 2):

$$\mu_i = \mu_i^0 + \mathrm{RT}\,\ln a_i \tag{2}$$

by replacing the expression of chemical potential into the expression of free Gibbs energy variation, we obtain Eq. 3:

$$\begin{aligned}\Delta G = {} & c(\mu_c^0 + \mathrm{RT}\,\ln a_C) + d(\mu_d^0 + \mathrm{RT}\,\ln a_d) - a(\mu_a^0 + \mathrm{RT}\,\ln a_a) \\ & - b(\mu_b^0 + \mathrm{RT}\,\ln a_b)\end{aligned} \tag{3}$$

or, it could be expressed as Eq. 4:

$$\Delta G = \Delta G^0 + \mathrm{RT}\,\ln \frac{a_c^c a_d^d}{a_a^a a_b^b} \tag{4}$$

But, the quantity of energy furnished by an electrochemical device into the external circuit in isotherm–isobar conditions is represented by Gibbs free energy variation of cell reaction [4, 6, 11, 15, 122, 123]:

$$W = \Delta G = -nFE \tag{5}$$

$$\rightarrow E = -\frac{1}{nF}\Delta G \tag{6}$$

where:

E electromotive force of the cell
n number of electrons involved into the cell reaction
F Faraday's Number
ΔG Gibbs free energy variation

From Eqs. 4 and 6, the following relation describing fuel cell electromotive force can be obtained:

$$E = -\frac{1}{nF}\Delta G^0 - \frac{\mathrm{RT}}{nF}\ln\frac{a_c^c a_d^d}{a_a^a a_b^b} \tag{7}$$

$$E = E^0 + \frac{\mathrm{RT}}{nF}\ln\frac{a_a^a a_b^b}{a_c^c a_d^d} \tag{8}$$

Let us evaluate the theoretical potential of a classical H_2/O_2 fuel cell. From Eq. 6, the maximum electrical output of a cell depends on the variation of Gibbs free energy, number of electrons involved in the reaction, and Faraday's Number [1, 4, 6, 8, 11, 15, 122]. In this particular case, considering the overall cell reaction as $H_2 + ½O_2 \rightarrow H_2O$, the Gibbs free energy can be expressed as (Eq. 9):

$$\Delta G = \Delta H - T\Delta S \tag{9}$$

where ΔH-change in enthalpy during reaction, and ΔS-change in entropy during reaction. Change in enthalpy can be expressed as [124]:

$$\Delta H = \int_{H_i}^{H_f} \mathrm{d}H = H_F - H_i \tag{10}$$

Suppose reaction takes place at 25 °C, at this temperature the standard heat of formation of liquid water is −286.02 kJ mol^{-1}, and that of H_2 and O_2 is zero [4, 124].

$$\Delta H^0 = H^0_{H_2O} - H^0_{H_2} - H^0_{O_2} = -286.02 - 0 - 0 = -286\,\text{kJ mol}^{-1} \tag{11}$$

Similarly, change in entropy for water formation can be estimated from Eq. 12 [4, 124]:

$$\begin{aligned}\Delta S^0 &= S^0_{H_2O} - S^0_{H_2} - \frac{1}{2}S^0_{O_2} = 0.06996 - 0.13066 - \frac{0.20517}{2} \\ &= -0.163285\,\text{kJ mol}^{-1}\text{K}^{-1}\end{aligned} \tag{12}$$

From Eqs. 11 and 12, the Gibbs free energy for water formation can be calculated [4, 124]:

$$\Delta G^0 = -286 - 298.15 \times (-0.163285) \tag{13}$$

$$\rightarrow \Delta G = -237.32\,\text{kJ mol}^{-1} \tag{14}$$

From Eq. 6, the maximum electromotive force of H_2/O_2 fuel cell can be estimated:

$$E = -\frac{\Delta G^0}{nF} = \frac{237.32 \times 10^3}{2 \times 96485} = 1.2298\,\text{V} \tag{15}$$

When the reaction products are in gaseous state, the cell voltage would be different. In this case, at 25 °C, heat of formation of water is $H^0_{H_2O} = -241.818$ kJ mol^{-1}, and entropy is $S^0_{H_2O} = 0.18882$ kJ mol^{-1} K^{-1} [124]. By using these values, changes in enthalpy and entropy can be calculated as:

$$\Delta H = -241.818\,\text{kJ mol}^{-1} \tag{16}$$

and

$$\Delta S = 0.044425\,\text{kJ mol}^{-1}\text{K}^{-1} \tag{17}$$

That means the Gibbs free energy is more positive: $\Delta G = -228.57$ kJ mol^{-1}. By using the new value of ΔG, it is possible to determine the maximum cell voltage when the water is in vapor form:

$$E = -\frac{\Delta G}{nF} = \frac{228.57 \times 10^3}{2 \times 96485} = 1.1845\,\text{V} \tag{18}$$

When the reaction product is in vapor form, the maximum cell voltage that can be obtained is lower than that with liquid reaction product. This difference between the two maximum cell voltages is associated with the Gibbs free energy consumed for the vaporization of water molecules [4, 6, 122, 124].

Since the cell voltage depends on Gibbs free energy, hence, all the parameters namely temperature, pressure and reactant concentration; influencing Gibbs free energy, affects cell voltage.

5.1 Effect of Temperature

Gibbs free energy is given by the difference between ΔH and $T\Delta S$. Enthalpy of a substance increases with increasing temperature. Change in enthalpy with change in temperature at constant pressure can be calculated as [124, 125]:

$$\Delta H = \int_{T_i}^{T_f} C_p \mathrm{d}T \tag{19}$$

Similarly, change in entropy can be expressed as [124, 125]:

$$\Delta S = \int_{T_i}^{T_f} \frac{C_p}{T} \mathrm{d}T. \tag{20}$$

Substituting Eqs. 19 and 20 in Eq. 9 we get

$$\Delta G = \int_{T_i}^{T_f} C_p \mathrm{d}T - T \int_{T_i}^{T_f} \frac{C_p}{T} \mathrm{d}T \tag{21}$$

Heat capacity itself is not a constant term and depends on temperature: $C_\mathrm{p} = f(T)$. An empirical expression for molar heat capacity is given by Eq. 22 [124, 125]:

$$C_p = a + bT + c\frac{1}{T^2} \tag{22}$$

where a, b, and c are empirical constants which are independent of temperature. By substituting Eq. 21 with Eqs. 19 and 20, we obtain the temperature dependence relationship among ΔG, ΔH, and ΔS.

Using the constants available in Atkins' Physical Chemistry [125], the values of ΔH, ΔS, and ΔG for different temperatures can be calculated. From the values of Gibbs free energy, enthalpy and entropy at different temperatures [124] the maximum theoretical fuel cell performance at a particular temperature can be estimated [1, 6, 124] as shown in Table 2.

Table 2 Estimated maximum fuel cell performance

Temperature (K)	E_{cell} (V)
298.15	1.229
333.15	1.200
353.15	1.184
373.15	1.167

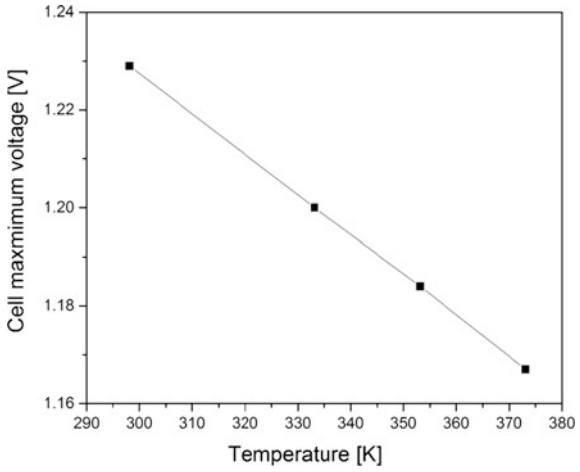

Fig. 5 Ideal potential of H_2/O_2 fuel cell as function of temperature

From Eq. 21 and Table 1, a strong dependence between the maximum voltage that can be obtained in a fuel cell and temperature of operation is evident. With increase of temperature, maximum cell voltage decreases as shown in Fig. 5.

5.2 *Effect of Pressure*

In order to evaluate the effect of pressure, the relationship of Gibbs free energy with pressure at constant temperature is important [4]. It is assumed that all gases involved are ideal gases. Applying the first and second laws of thermodynamics for a reversible reaction, the relationship between entropy and enthalpy can be obtained [124, 125]:

$$T\mathrm{d}S = \mathrm{d}H - V\mathrm{d}P \tag{23}$$

Enthalpy is an extensive quantity which depends on temperature and pressure:

$$\mathrm{d}H = \left(\frac{\partial H}{\partial T}\right)_P \mathrm{d}T + \left(\frac{\partial H}{\partial P}\right)_T \mathrm{d}P \tag{24}$$

By substituting Eq. 24 in Eq. 23:

$$T\mathrm{d}S = \left(\frac{\partial H}{\partial T}\right)_P \mathrm{d}T + \left(\frac{\partial H}{\partial P}\right)_T \mathrm{d}P - V\mathrm{d}P \tag{25}$$

Substituting $C_P = \left(\frac{\partial H}{\partial T}\right)_P$:

$$\mathrm{d}S = \frac{1}{T} C_P \mathrm{d}T + \frac{1}{T}\left[\left(\frac{\partial H}{\partial P}\right)_T - V\right]\mathrm{d}P \tag{26}$$

By definition of prefect gases, enthalpy is only a function of temperature, that is $\left(\frac{\partial H}{\partial P}\right)_T = 0$, hence Eq. 26 becomes:

$$\mathrm{d}S = \frac{1}{T} C_P \mathrm{d}T - \frac{1}{T} V\mathrm{d}P \tag{27}$$

using the perfect gase state:

$$\mathrm{d}S = \frac{C_P}{T}\mathrm{d}T - R\frac{\mathrm{d}P}{P} \tag{28}$$

$$\Delta S = C_p \ln\frac{T}{T_0} - R \ln\frac{P}{P_0} \tag{29}$$

Similarly change in enthalpy can be obtained as:

$$\Delta H = C_P(T - T_0) \tag{30}$$

By substituting Eqs. 29 and 30 in Eq. 9:

$$\Delta G = \left(C_P - S^0\right)(T - T_0) - C_p T \ln\frac{T}{T_0} + \mathrm{RT} \ln\frac{P}{P_0} \tag{31}$$

From the above equations, the variation of Gibbs free energy with pressure can be obtained as [4]:

$$\Delta G = \left[\sum_i n_i C_{p,i} - \sum_i n_i S_{i,0}\right](T - T_0) - \left(\sum_i n_i C_{p,i}\right) T \ln\frac{T}{T_0} + \mathrm{RT}\sum_i {}' n_i \ln\frac{p_i}{p_{i,0}}, \tag{32}$$

where G—Gibbs free energy, C_p—molar heat at constant pressure, S—entropy, P—pressure, and T—temperature.

By substituting ΔG value in Eq. 6, Nernst Equation can be obtained [4, 6]:

$$E = E^0 + \frac{\mathrm{RT}}{nF} \ln \frac{P_{\mathrm{H_2}} P_{\mathrm{O_2}}^{1/2}}{P_{\mathrm{H_2O}}} \tag{33}$$

When water is present in liquid form, it is necessary to replace the partial pressure of water with 1. In this case, we can conclude that the increase of reactant pressure leads to an increase of fuel cell potential.

5.3 *Effect of Concentration of Reactant*

Concentration of reactants also affects cell voltage. For example in a H_2/O_2 fuel cell, if air is used instead of pure oxygen, there will be a drop in performance. The partial pressure of a gas is proportional to its concentration in the gas mixture. Since, partial pressure of oxygen in air is only 0.21 of that of pure oxygen which results in a decreased cell voltage when air is used instead of pure oxygen.

6 Fuel Cell Efficiency

Thermal efficiency of any conversion device is defined as the ratio between the quantity of useful energy produced and the energy input. This energy input can be evaluated as the change in enthalpy between the products and reactants [1, 4, 6, 8, 122]. Classical conversion devices use thermo-mechanical conversion systems, in which the maximum efficiency is limited by the initial and final temperatures of the fluid [4, 6]. For electrochemical devices which convert chemical energy directly into electrical energy, the produced electrical energy can be calculated directly from the Gibbs free energy:

$$\eta_{\max}[\%] = \frac{\Delta G}{\Delta H} \times 100 \tag{33}$$

Under standard conditions (298 K temperature and 1 atmospheric pressure), thermal energy for overall reaction in a H_2/O_2 fuel cell is $\Delta H = -286\,\mathrm{kJ\ mol^{-1}}$, and the free Gibbs energy is $\Delta G = -237.32\,\mathrm{kJ\ mol^{-1}}$. By substituting these values in Eq. 33, the maximum cell efficiency can be obtained under standard conditions:

$$\eta_{\max}[\%] = \frac{-237.32\,\mathrm{kJ\ mol^{-1}}}{-286\,\mathrm{kJ\ mol^{-1}}} \times 100 = 82.98\% \tag{34}$$

6.1 Losses in Actual System

The actual cell potential obtained during operation of a fuel cell is less than the ideal theoretical potential at standard conditions. This is due to polarization taking place at the electrodes. These polarizations are known as overpotential or overvoltage [4, 6], and they are dependent on the fuel cell load, which are classified into three types:

- activation overpotential;
- ohmic polarization losses;
- mass transport overpotential.

6.2 Activation Overpotential

It appears at lower values of current density, as a consequence of low electrode kinetics. Such overpotential appears when the electrochemical reaction speed is controlled by charge transfer. Activation overpotential can also be influenced by the nature of the electrode, adsorption of the reactants on electrode surface, and the slow reaction kinetics between adsorbed intermediates. Activation overpotential can be calculated by Tafel equation, obtained as a particularization of Butler–Volmer Equation [4].

For the anodic reaction activation overpotential can be expressed as:

$$\eta_{\text{act}}^{a} = \frac{\text{RT}}{\alpha z F} \ln \frac{i}{i_0} \tag{35}$$

Similarly for the cathodic reaction activation overpotential can be expressed as:

$$\eta_{\text{act}}^{c} = \frac{\text{RT}}{(1-\alpha) z F} \ln \frac{i}{i_0} \tag{36}$$

where α—anodic electron transfer coefficient, $1-\alpha$—cathodic electron transfer coefficient, i_0—exchange current density.

6.3 Ohmic Polarization Losses

These losses occur due to the resistance encountered by the ionic flow while passing through the electrolyte and the resistance encountered by the electrons when they pass through cell electrodes. The ohmic losses are directly related to the internal resistance of the electrolyte, and can be reduced by increasing the ionic

conduction of the polymeric membrane, as well as also by reducing the distance between anode and cathode (reducing the thickness of the membrane). Ohmic losses also depend on the internal resistance of the electrodes. Experimental data confirm that the electrolyte and the electrodes obey Ohm's Law (Eq. 37):

$$\eta_{\text{ohm}} = IR \tag{37}$$

6.4 Mass Transport Overpotential

It appears because the reaction actually takes place at the electrode–electrolyte interface. Consumption of the reactants reduces the availability of reacting species at the electrode surface. At the same time, presence of reaction products at the interface reduces the concentration of active reaction species. Hence, a concentration gradient is formed between the electrode surface and bulk liquid which causes mass transport overpotential.

Mass transport overpotential is caused because of:

- slow diffusion of gaseous phase into the active reaction sites;
- slow reactants and products diffusion through electrolyte to and from the place where the electrochemical reaction occurs;
- slow dissolution of reactants and reaction products into the electrolyte.

As a consequence of the concentration gradient, a sharp variation of the cell potential appears under practical conditions especially at high current densities, low fuel concentration, and low oxidant concentration, representing a significant loss of the cell potential. At practical current densities observed in fuel cells, the reactants are supplied at electrodes by diffusion; hence, the rate of mass transport can be described by Fick's Law of diffusion (Eq. 38):

$$\eta_{\text{diff}} = \frac{\text{RT}}{zF} \ln\left(1 - \frac{j}{j_{\text{lim}}}\right) \tag{38}$$

where j_{lim}—diffusion limiting current.

Activation and mass transport overpotentials can appear at both anode and cathode:

$$\eta_{\text{anode}} = \eta_{\text{act,anod}} + \eta_{\text{conc,anod}} \tag{39}$$

$$\eta_{\text{cathode}} = \eta_{\text{act,cathode}} + \eta_{\text{conc,cathode}} \tag{40}$$

Hence, the anode potential becomes more positive and the cathode potential becomes more negative as compared to ideal conditions:

$$E_{\text{anod}} = E_{\text{anod}} + \eta_{\text{anod}} \tag{41}$$

$$E_{\text{cathode}} = E_{\text{cathode}} - |\eta_{\text{cathode}}| \tag{42}$$

From the above equations overall cell potential can be estimated as:

$$E_{\text{cel}} = E_{\text{cathode}} - |\eta_{\text{cathode}}| - (E_{\text{anod}} + \eta_{\text{anod}}) - iR \tag{43}$$

$$E_{\text{cel},I\neq 0} = E_{\text{rev}} - \sum |\eta| - iR \tag{44}$$

When a cell is delivering energy to the external circuit; increase of current density leads to a decrease of cell voltage, due to activation, concentration and ohmic polarization losses. Future research must focus on minimization of all these internal losses in order to get a closer value of $E_{\text{cel},I\neq 0}$ to the cell reversible potential.

7 Conclusion

Fuel cells represent a viable option for clean energy production by direct conversion of chemical energy into electrical energy. Maximum theoretical cell voltage obtained for direct conversion of hydrogen is 1.2298 V with a cell efficiency of 82.98%. Due to several losses the real cell performance obtained during system operation is less than the ideal theoretical cell performance at standard conditions. The cell voltage is dependent on Gibbs free energy and in turn on: temperature, pressure, and partial pressure of reactants. Future research should deal with minimization of all internal losses in order to increase the real cell potential to a closer value to the theoretical cell potential.

References

1. Barbir F (2005) PEM fuel cells: theory and practice. Elsevier Academic Press
2. Energy USDo (2013) Fuel cell technologies overview (cited 10 Mar 2016)
3. History NMoA (cited 2016 15.04.2016); Available from: http://americanhistory.si.edu/fuelcells/origins/origins.htm
4. Oniciu L (1976) Fuel cells. Abacus Press
5. Scott K et al (2012) Biological and microbial fuel cells. In: Sayigh A (ed) Comprehensive renewable energy. Elsevier, Amsterdam, pp 257–280
6. EG&G Technical Services I (2004) Fuel cell handbook, 7th edn. U.S. Department of Energy, Morgantown, West Virginia 26507 - 0880
7. Mekhilef S, Saidur R, Safari A (2012) Comparative study of different fuel cell technologies. Renew Sustain Energy Rev 16(1):981–989
8. Kirubakaran A, Jain S, Nema RK (2009) A review on fuel cell technologies and power electronic interface. Renew Sustain Energy Rev 13(9):2430–2440

9. Merle G, Wessling M, Nijmeijer K (2011) Anion exchange membranes for alkaline fuel cells: a review. J Membr Sci 377(1–2):1–35
10. Liu Y et al (2016) A review of high-temperature polymer electrolyte membrane fuel-cell (HT-PEMFC)-based auxiliary power units for diesel-powered road vehicles. J Power Sources 311:91–102
11. Lepiller C (2016) Fuel cell basics. Available from: http://www.pragma-industries.com/wp-content/themes/default/images/fuel_cell_basics.pdf
12. Cao D, Sun Y, Wang G (2007) Direct carbon fuel cell: fundamentals and recent developments. J Power Sources 167(2):250–257
13. Duteanu N et al (2007) A parametric study of a platinum ruthenium anode in a direct borohydride fuel cell. J Appl Electrochem 37(9):1085–1091
14. Scott K et al (2008) Performance of a direct methanol alkaline membrane fuel cell. J Power Sources 175(1):452–457
15. Sharaf OZ, Orhan MF (2014) An overview of fuel cell technology: Fundamentals and applications. Renew Sustain Energy Rev 32:810–853
16. Srinivasan S et al (1991) Proceedings of the third space electrochemical research and technology conference. High energy efficiency and high power density proton exchange membrane fuel cells–electrode kinetics and mass transport. J Power Sources 36(3):299–320
17. Straßer K (1990) PEM-fuel cells: state of the art and development possibilities. Ber Bunsenges Phys Chem 94(9):1000–1005
18. Gurau V et al (2007) Characterization of transport properties in gas diffusion layers for proton exchange membrane fuel cells: 2. Absolute permeability. J Power Sources 165(2): 793–802
19. Prater KB (1992) Proceedings of the second Grove fuel cell symposium. Progress in fuel cell commercialisation. Solid polymer fuel cell developments at Ballard. J Power Sources 37(1): 181–188
20. Wilson MS, Gottesfeld S (1992) Thin-film catalyst layers for polymer electrolyte fuel cell electrodes. J Appl Electrochem 22(1):1–7
21. Wasmus S, Küver A (1999) Methanol oxidation and direct methanol fuel cells: a selective review. J Electroanal Chem 461(1–2):14–31
22. Biyikoglu A (2005) Review of proton exchange membrane fuel cell models. Int J Hydrogen Energy 30(11):1181–1212
23. Strasser K (1992) Proceedings of the second Grove fuel cell symposium. Progress in fuel cell commercialisation. Mobile fuel cell development at Siemens. J Power Sources 37(1):209–219
24. Wang ZH, Wang CY, Chen KS (2001) Two-phase flow and transport in the air cathode of proton exchange membrane fuel cells. J Power Sources 94(1):40–50
25. Gurau V et al (2006) Characterization of transport properties in gas diffusion layers for proton exchange membrane fuel cells: 1. Wettability (internal contact angle to water and surface energy of GDL fibers). J Power Sources 160(2):1156–1162
26. Zhou W et al (2003) Pt based anode catalysts for direct ethanol fuel cells. Appl Catal B 46 (2):273–285
27. Shukla S et al (2015) Analysis of low platinum loading thin polymer electrolyte fuel cell electrodes prepared by inkjet printing. Electrochim Acta 156:289–300
28. Oh H-S et al (2009) Corrosion resistance and sintering effect of carbon supports in polymer electrolyte membrane fuel cells. Electrochim Acta 54(26):6515–6521
29. Alcaide F et al (2009) Pt supported on carbon nanofibers as electrocatalyst for low temperature polymer electrolyte membrane fuel cells. Electrochem Commun 11(5): 1081–1084
30. Guha A et al (2007) Surface-modified carbons as platinum catalyst support for PEM fuel cells. Carbon 45(7):1506–1517
31. Subramanian NP et al (2009) Nitrogen-modified carbon-based catalysts for oxygen reduction reaction in polymer electrolyte membrane fuel cells. J Power Sources 188(1):38–44
32. Calvillo L et al (2009) Effect of the support properties on the preparation and performance of platinum catalysts supported on carbon nanofibers. J Power Sources 192(1):144–150

33. Calvillo L et al (2007) Platinum supported on functionalized ordered mesoporous carbon as electrocatalyst for direct methanol fuel cells. J Power Sources 169(1):59–64
34. Sebastian D et al (2009) Carbon nanofibers as electrocatalyst support for fuel cells: effect of hydrogen on their properties in CH4 decomposition. J Power Sources 192(1):51–56
35. Andersen SM et al (2013) Durability of carbon nanofiber (CNF) & carbon nanotube (CNT) as catalyst support for proton exchange membrane fuel cells, pp 94–101
36. Sebastian D et al (2010) Influence of carbon nanofiber properties as electrocatalyst support on the electrochemical performance for PEM fuel cells. Int J Hydrogen Energy 35(18): 9934–9942
37. Li YH et al (2016) Preparation of platinum catalysts supported on functionalized graphene and the electrocatalytic properties for ethanol oxidation in direct ethanol fuel cell. J Mater Sci Mater Electron 27(6):6208–6215
38. Peighambardoust SJ, Rowshanzamir S, Amjadi M (2010) Review of the proton exchange membranes for fuel cell applications. Int J Hydrogen Energy 35(17):9349–9384
39. An L, Chen R (2016) Direct formate fuel cells: a review. J Power Sources 320:127–139
40. Antolini E, Gonzalez ER (2010) Alkaline direct alcohol fuel cells. J Power Sources 195(11): 3431–3450
41. Rimbu GA, Jackson CL, Scott K (2006) Platinum/carbon/polyaniline based nanocomposites as catalysts for fuel cell technology. J Optoelectron Adv Mater 8(2):611–616
42. Zhao TS, Li YS, Shen SY (2010) Anion-exchange membrane direct ethanol fuel cells: Status and perspective. Front Energy Power Eng Chin 4(4):443–458
43. Zheng Y et al (2016) Platinum nanoparticles on carbon-nanotube support prepared by room-temperature reduction with H_2 in ethylene glycol/water mixed solvent as catalysts for polymer electrolyte membrane fuel cells, 448–453
44. Antolini E (2015) Composite materials for polymer electrolyte membrane microbial fuel cells. Biosens Bioelectron 69:54–70
45. Bayatsarmadi B, Peters A, Talemi P (2016) Catalytic polymeric electrodes for direct borohydride fuel cells. J Power Sources 322:26–30
46. Cheddie D, Munroe N (2005) Review and comparison of approaches to proton exchange membrane fuel cell modeling. J Power Sources 147(1–2):72–84
47. Giddey S et al (2012) A comprehensive review of direct carbon fuel cell technology. Prog Energy Combust Sci 38(3):360–399
48. Indig ME, Snyder RN (1962) Sodium borohydride, an interesting anodic fuel (1). J Electrochem Soc 109(11):1104–1106
49. Iwan A, Malinowski M, Pasciak G (2015) Polymer fuel cell components modified by graphene: Electrodes, electrolytes and bipolar plates. Renew Sustain Energy Rev 49: 954–967
50. Carrette L, Friedrich KA, Stimming U (2001) Fuel cells—fundamentals and applications. Fuel Cells 1(1):5–39
51. Divisek J et al (1998) Components for PEM fuel cell systems using hydrogen and CO containing fuels. Electrochim Acta 43(24):3811–3815
52. Litster S, McLean G (2004) PEM fuel cell electrodes. J Power Sources 130(1–2):61–76
53. Cindrella L et al (2009) Gas diffusion layer for proton exchange membrane fuel cells—a review. J Power Sources 194(1):146–160
54. Oedegaard A et al (2004) Influence of diffusion layer properties on low temperature DMFC. J Power Sources 127(1–2):187–196
55. Neergat M, Shukla AK (2002) Effect of diffusion-layer morphology on the performance of solid-polymer-electrolyte direct methanol fuel cells. J Power Sources 104(2):289–294
56. Feser JP, Prasad AK, Advani SG (2006) Experimental characterization of in-plane permeability of gas diffusion layers. J Power Sources 162(2):1226–1231
57. Song M, Kim HY, Kim K (2014) Effects of hydrophilic/hydrophobic properties of gas flow channels on liquid water transport in a serpentine polymer electrolyte membrane fuel cell. 19714–19721
58. Zhang J et al (2006) High temperature PEM fuel cells. J Power Sources 160(2):872–891

59. Pan YH (2006) Advanced air-breathing direct methanol fuel cells for portable applications. J Power Sources 161(1):282–289
60. Escribano S, Aldebert P (1995) Electrodes for hydrogen/oxygen polymer electrolyte membrane fuel cells. Solid State Ionics 77:318–323
61. Fischer A, Jindra J, Wendt H (1998) Porosity and catalyst utilization of thin layer cathodes in air operated PEM-fuel cells. J Appl Electrochem 28(3):277–282
62. Chandan A et al (2013) High temperature (HT) polymer electrolyte membrane fuel cells (PEMFC)—a review. J Power Sources 231:264–278
63. Escribano S, Aldebert P (1995) Solid state protonic conductors vii electrodes for hydrogen/oxygen polymer electrolyte membrane fuel cells. Solid State Ionics 77:318–323
64. Shao Y et al (2007) Proton exchange membrane fuel cell from low temperature to high temperature: material challenges. J Power Sources 167(2):235–242
65. Liang Y et al (2006) Preparation and characterization of carbon-supported PtRuIr catalyst with excellent CO-tolerant performance for proton-exchange membrane fuel cells. J Catal 238(2):468–476
66. George MG et al (2016) Composition analysis of a polymer electrolyte membrane fuel cell microporous layer using scanning transmission X-ray microscopy and near edge X-ray absorption fine structure analysis. J Power Sources 309:254–259
67. Lobato J et al (2008) Influence of the teflon loading in the gas diffusion layer of PBI-based PEM fuel cells. J Appl Electrochem 38(6):793–802
68. Guo Z, Faghri A (2006) Development of planar air breathing direct methanol fuel cell stacks. J Power Sources 160(2):1183–1194
69. Bose S et al (2011) Polymer membranes for high temperature proton exchange membrane fuel cell: Recent advances and challenges. Prog Polym Sci 36(6):813–843
70. Fathirad F, Afzali D, Mostafavi A (2016) Pd-Zn nanoalloys supported on Vulcan XC-72R carbon as anode catalysts for oxidation process in formic acid fuel cell
71. Chu YH, Shul YG (2010) Combinatorial investigation of Pt-Ru-Sn alloys as an anode electrocatalysts for direct alcohol fuel cells. Int J Hydrogen Energy 35(20):11261–11270
72. Kim HS et al (2016) Platinum catalysts protected by N-doped carbon for highly efficient and durable polymer-electrolyte membrane fuel cells. Electrochim Acta (in press)
73. Jongsomjit S, Prapainainar P, Sombatmankhong K (2016) Synthesis and characterisation of Pd-Ni-Sn electrocatalyst for use in direct ethanol fuel cells. Solid State Ionics 288:147–153
74. Arashi T et al (2014) Nb-doped TiO_2 cathode catalysts for oxygen reduction reaction of polymer electrolyte fuel cells. Catal Today Catal Mater Catal Low Carbon Technol 233:181–186
75. Han S, Chae GS, Lee JS (2016) Enhanced activity of carbon-supported PdCo electrocatalysts toward electrooxidation of ethanol in alkaline electrolytes. Korean J Chem Eng 33 (6):1799–1804
76. Kumar A, Ramani VK (2013) RuO_2-SiO_2 mixed oxides as corrosion-resistant catalyst supports for polymer electrolyte fuel cells. Appl Catal B 138–139:43–50
77. Patru A et al (2016) Pt/IrO_2–TiO_2 cathode catalyst for low temperature polymer electrolyte fuel cell—application in MEAs, performance and stability issues. Catal Today 262:161–169
78. Uehara N et al (2015) Tantalum oxide-based electrocatalysts made from oxy-tantalum phthalocyanines as non-platinum cathodes for polymer electrolyte fuel cells. Ubiquitus Electrochem 146–153
79. Yi L et al (2015) Enhanced activity of Au-Fe/C anodic electrocatalyst for direct borohydride-hydrogen peroxide fuel cell. J Power Sources 285:325–333
80. Kil KC et al (2014) The use of MWCNT to enhance oxygen reduction reaction and adhesion strength between catalyst layer and gas diffusion layer in polymer electrolyte membrane fuel cell. Int J Hydrogen Energy 39:17481–17486
81. Chen Z et al (2011) A review on non-precious metal electrocatalysts for PEM fuel cells. Energy Environ Sci 4(9):3167–3192
82. Reshetenko TV, Kim H-T, Kweon H-J (2007) Cathode structure optimization for air-breathing DMFC by application of pore-forming agents. J Power Sources 171(2):433–440

83. Wang B (2005) Recent development of non-platinum catalysts for oxygen reduction reaction. J Power Sources 152:1–15
84. Kinumoto T et al (2006) Durability of perfluorinated ionomer membrane against hydrogen peroxide. J Power Sources 158(2):1222–1228
85. Smitha B, Sridhar S, Khan AA (2005) Solid polymer electrolyte membranes for fuel cell applications—a review. J Membr Sci 259(1–2):10–26
86. Prater KB (1994) Polymer electrolyte fuel cells: a review of recent developments. J Power Sources 51(1):129–144
87. Sousa R Jr, Gonzalez ER (2005) Mathematical modeling of polymer electrolyte fuel cells. J Power Sources 147(1–2):32–45
88. Owejan JP et al (2007) Effects of flow field and diffusion layer properties on water accumulation in a PEM fuel cell. Int J Hydrogen Energy 32(17):4489–4502
89. Neburchilov V et al (2007) A review of polymer electrolyte membranes for direct methanol fuel cells. J Power Sources 169(2):221–238
90. DuPont (2016) Nafion—product bulletin P-12 (cited 10 May 2016). Available from: https://www.chemours.com/Nafion/en_US/assets/downloads/nafion-extrusion-cast-membranes-product-information.pdf
91. Yu EH, Scott K (2004) Development of direct methanol alkaline fuel cells using anion exchange membranes. J Power Sources 137(2):248–256
92. Yu EH, Scott K (2005) Direct methanol alkaline fuel cells with catalysed anion exchange membrane electrodes. J Appl Electrochem 35(1):91–96
93. Lim BH et al (2016) Effects of flow field design on water management and reactant distribution in PEMFC: a review. Ionics 22(3):301–316
94. Nguyen TV (1996) A gas distributor design for proton—exchange—membrane fuel cells. J Electrochem Soc 143(5):L103–L105
95. Rostami L, Mohamad Gholy Nejad P, Vatani A (2016) A numerical investigation of serpentine flow channel with different bend sizes in polymer electrolyte membrane fuel cells. Energy 97:400–410
96. Baek SM et al (2012) Pressure drop and flow distribution characteristics of single and parallel serpentine flow fields for polymer electrolyte membrane fuel cells. J Mech Sci Technol 26(9):2995–3006
97. Hsieh S-S, Her B-S, Huang Y-J (2011) Effect of pressure drop in different flow fields on water accumulation and current distribution for a micro PEM fuel cell. Energy Convers Manag 52(2):975–982
98. Yang H, Zhao TS, Ye Q (2005) Pressure drop behavior in the anode flow field of liquid feed direct methanol fuel cells. J Power Sources 142(1–2):117–124
99. Cho K-S (2015) The flow-field pattern optimization of the bipolar plate for PEMFC considering the nonlinear material. Int J Electrochem Sci 10:2564–2579
100. Beale SB (2015) Mass transfer formulation for polymer electrolyte membrane fuel cell cathode. Int J Hydrogen Energy 40:11641–11650
101. Diedrichs A et al (2013) Effect of compression on the performance of a HT-PEM fuel cell. J Appl Electrochem 43(11):1079–1099
102. Choi K-S, Kim H-M, Moon S-M (2011) Numerical studies on the geometrical characterization of serpentine flow-field for efficient PEMFC. Int J Hydrogen Energy 36(2):1613–1627
103. Arvay A et al (2013) Nature inspired flow field designs for proton exchange membrane fuel cell. Int J Hydrogen Energy 38(9):3717–3726
104. Li X, Sabir I (2005) Review of bipolar plates in PEM fuel cells: Flow-field designs. Int J Hydrogen Energy 30(4):359–371
105. Wang J, Wang H (2012) Flow-field designs of bipolar plates in pem fuel cells: theory and applications. Fuel Cells 12(6):989–1003
106. Aricò AS, Baglio V, Antonucci V (2009) Direct methanol fuel cells: history, status and perspectives. In: Electrocatalysis of direct methanol fuel cells. Wiley-VCH Verlag GmbH & Co. KGaA, pp 1–78

107. Aricò AS, Srinivasan S, Antonucci V (2001) DMFCs: from fundamental aspects to technology development. Fuel Cells 1(2):133–161
108. Yu X, Pickup PG (2008) Recent advances in direct formic acid fuel cells (DFAFC). J Power Sources 182(1):124–132
109. Demirci UB (2007) Direct liquid-feed fuel cells: thermodynamic and environmental concerns. J Power Sources 169(2):239–246
110. Kamarudin MZF et al (2013) Review: direct ethanol fuel cells. Int J Hydrogen Energy 38 (22):9438–9453
111. Lamy C, Coutanceau C, Leger JM (2009) The direct ethanol fuel cell: a challenge to convert bioethanol cleanly into electric energy. In: Catalysis for sustainable energy production. Wiley-VCH Verlag GmbH & Co. KGaA, pp 1–46
112. An L et al (2010) Performance of a direct ethylene glycol fuel cell with an anion-exchange membrane. Int J Hydrogen Energy 35(9):4329–4335
113. Modestov AD et al (2009) MEA for alkaline direct ethanol fuel cell with alkali doped PBI membrane and non-platinum electrodes. J Power Sources 188(2):502–506
114. Fujiwara N et al (2008) Direct ethanol fuel cells using an anion exchange membrane. J Power Sources 185(2):621–626
115. An L et al (2011) Alkaline direct oxidation fuel cell with non-platinum catalysts capable of converting glucose to electricity at high power output. J Power Sources 196(1):186–190
116. An L, Zhao TS, Xu JB (2011) A bi-functional cathode structure for alkaline-acid direct ethanol fuel cells. Int J Hydrogen Energy 36(20):13089–13095
117. Ha S, Dunbar Z, Masel RI (2006) Characterization of a high performing passive direct formic acid fuel cell. J Power Sources 158(1):129–136
118. Jeong K-J et al (2007) Fuel crossover in direct formic acid fuel cells. J Power Sources 168(1): 119–125
119. Miesse CM et al (2006) Direct formic acid fuel cell portable power system for the operation of a laptop computer. J Power Sources 162(1):532–540
120. Rice C et al (2002) Direct formic acid fuel cells. J Power Sources 111(1):83–89
121. Boyaci San FG et al (2014) Evaluation of operating conditions on DBFC (direct borohydride fuel cell) performance with PtRu anode catalyst by response surface method. Energy 71:160–169
122. Lucia U (2014) Overview on fuel cells. Renew Sustain Energy Rev 30:164–169
123. Mahapatra MK, Singh P (2014) Fuel cells: energy conversion technology A2. In: Letcher TM (ed) Future energy, 2nd edn (Chap. 24). Elsevier, Boston, pp 511–547
124. Davidescu CM (2002) Introducere in termodinamica chimica. Editura Politehnica, Timisoara
125. Atkins P, de Paula J (2005) Atkins' physical chemistry. Oxford University Press